Electronic Supplementary Material (ESI) for Journal of Materials Chemistry C.


# Isomeric ligand enhancing the anisotropy barrier within nine-coordinated {Dy2} Compounds

Lin Sun‡[a], Shilong Wei‡[a], Jun Zhang[c], Wenyuan Wang[a], Sanping Chen*[a], Yiquan Zhang*[b], Qing Wei[a], Gang Xie[a], Shengli Gao[a]

[a.] *Key Laboratory of Synthetic and Natural Functional Molecule Chemistry of Ministry of Education, College of Chemistry and Materials Science, Northwest University, Xi'an, Shaanxi 710127, China.*

[b.] *Jiangsu Key Laboratory for NSLSCS, School of Physical Science and Technology, Nanjing Normal University, Nanjing 210023, China*

[c.] *School of Materials and Chemical Engineering, Anhui Jianzhu University, Hefei, 230601, China*

‡ These authors contributed equally to this work.

***Corresponding authors**

**Dr. Sanping Chen, Dr. Yi-Quan Zhang**

**E-mail address: sanpingchen@126.com; zhangyiquan@njnu.edu.cn**

# Contents

## Quantum chemical calculation for 2,3′-Hpcad and 2,4′-Hpcad

Theoretical research on the electronic configuration for 2,3′-Hpcad and 2,4′-Hpcad was carried out using Gaussian09 program [S1], at the B3LYP [S2,S3] level of theory with 6-31G(d, p) basis set.

Density function theory (DFT) method was performed to get an insight of the electronic structures and bonding properties of 2,3′-Hpcad and 2,4′-Hpcad. The following calculation and discussion are resulted from the optimized structure. The full geometry optimization is performed without constraints on symmetry. The optimized geometries of different conformations have been obtained at the B3LYP/6-31G(d, p) level and shown in Figure S1.

The molecular total energies, zero-point energies and frontier orbital energies and the energy gaps of different conformations had been calculated and listed in Table S1. For 2,3′-Hpcad, the total energies of four different conformations are calculated to be -812.6270, -812.6436, -812.6455, -812.6441 a.u., respectively. Obviously, the *trans*-I conformation provides relatively lower energy, representing more stable geometry. Compared with the *trans*-I conformation, the *cis*-I conformation (-812.6270 a.u.) of 2,4′-Hpcad shows more stable geometry.

The surfaces of HOMO-1, HOMO, LUMO and LUMO+1 for four conformations are shown in Figure S2. The frontier molecular orbitals of six conformations are mainly composed of *p* atomic orbitals, and the electronic *trans*itions are mainly assigned to $n \rightarrow \pi^*$ and $\pi \rightarrow \pi^*$ electronic *trans*itions. The same electron distribution of the frontier orbitals indicates similar electronic *trans*ition model. For 2,3′-Hpcad and 2,4′-Hpcad, the energy gaps of *trans*-I conformation ($\Delta E_{(\text{LUMO-HOMO})}$ = 4.24 eV) and *cis*-I conformation are lower than that of other conformations, respectively, suggesting the greater ability of electron *trans*ition under external stimuli. To estimate the possible coordinated condition of the *trans*-I conformation (2,3′-Hpcad) and *cis*-I conformation (2,4′-Hpcad), the natural charges and electron configurations of the atoms have been calculated by using natural bond orbital (NBO) analysis. As shown in Table S2, mulliken charges and natural charges of N1, N2, N3, N4, N5 and O1 atoms are calculated as negative values. However, N1, N2, N5 and O1 atoms of 2,3′-Hpcad with *d* Orbital contribution are prone to coordinate with metal ions. In particular, N1, N2 and O1 atoms of 2,3′-Hpcad (N3, N5 and O1 atoms of 2,4′-Hpcad) are more likely to coordinate to the metallic ions in tridentate-fashion. The position of N atoms in the pyridine ring is different (N5 of 2,3′-Hpcad; N1 of 2,4′-Hpcad), such subtle changes likely to fine-tine coordination geometry.

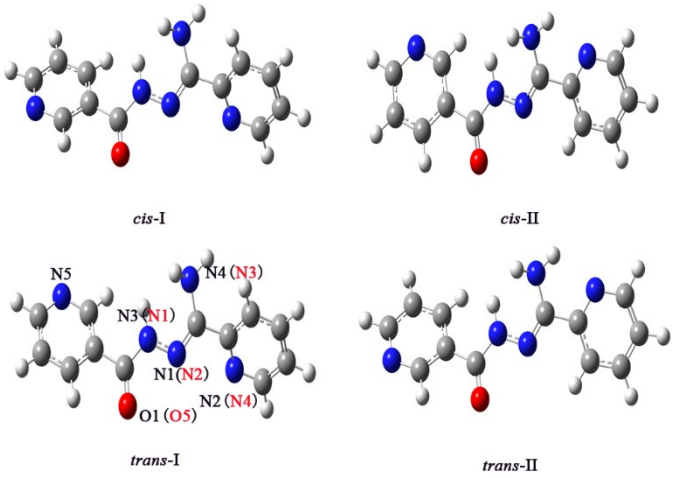


**Figure S1.** Optimized structures of four conformations for 2,3′-Hpcad.

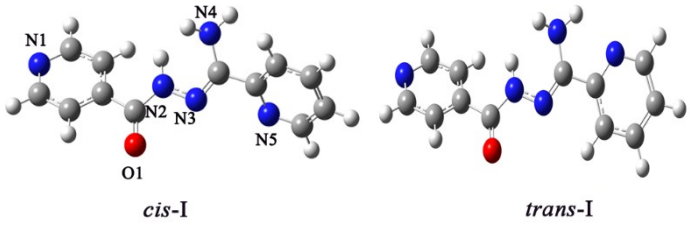


**Figure S2.** Optimized structures of four conformations for 2,4′-Hpcad.

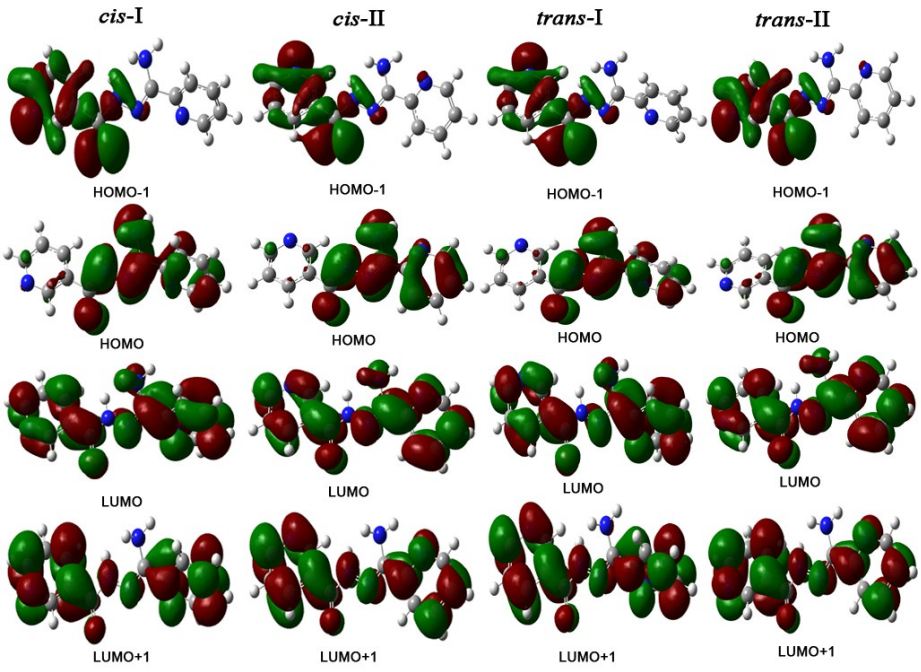


**Figure S3.** Isodensity surfaces of HOMO-1, HOMO, LUMO and LUMO+1 for 2,3′-Hpcad.

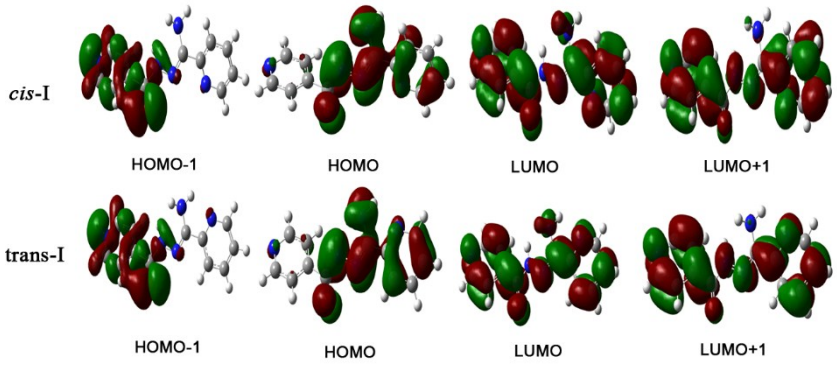


**Figure S4.** Isodensity surfaces of HOMO-1, HOMO, LUMO and LUMO+1 for 2,4′-Hpcad.

**Table S1.** Calculated total energies, zero-point energies and frontier orbit energies of 2,3′-Hpcad and 2,4′-Hpcad.

| | 2,3′-Hpcad | | | 2,4′-Hpcad | | |
|---|---|---|---|---|---|---|
| | *Cis*-I | *Cis*-II | ***Trans*-I** | *Trans*-II | ***Cis*-I** | *Cis*-II |
| $E$ / a.u. | -812.6270 | -812.6436 | **-812.6455** | -812.6441 | **-812.6445** | -812.6275 |
| ($E$+$ZPE$) / a.u. | -812.6422 | -812.6285 | **-812.6604** | -812.6590 | **-812.6594** | -812.6426 |
| $E_{(HOMO-1)}$ / a.u. | -0.24423 | -0.24562 | **-0.24824** | -0.24691 | **-0.25278** | -0.25006 |
| $E_{HOMO}$ / a.u. | -0.21631 | -0.21536 | **-0.21477** | -0.21580 | **-0.21794** | -0.21852 |
| $E_{LUMO}$ / a.u. | -0.05579 | -0.05535 | **-0.05894** | -0.05959 | **-0.06354** | -0.05959 |
| $E_{(LUMO+1)}$ / a.u. | -0.03760 | -0.03638 | **-0.03733** | -0.03882 | **-0.04233** | -0.04113 |
| $\Delta E_{(LUMO-HOMO)}$ / eV | 4.37 | 4.34 | **4.24** | 4.25 | **4.20** | 4.31 |

**Table S2.** Natural configurations and natural charges for the selected atoms of *tran*-I (2,3′-Hpcad) and *cis*-I (2,4′-Hpcad).

| Atom | Configuration | Natural charge | Mulliken charge |
|---|---|---|---|
| *Trans*-I (2,3′-Hpcad) | | | |
| **N1** | **[core]2*s*( 1.39)2*p*( 3.84)3*p*( 0.01)3*d*( 0.01)** | **-0.25511** | **-0.267946** |
| **N2** | **[core]2*s*( 1.37)2*p*( 4.03)3*p*( 0.01)3*d*( 0.01)** | **-0.41442** | **-0.443858** |
| N3 | [core]2*s*( 1.26)2*p*( 4.21)3*p*( 0.01) | -0.48192 | -0.438926 |
| N4 | [core]2*s*( 1.37)2*p*( 4.52)3*p*( 0.01) | -0.90090 | -0.655380 |
| **N5** | **[core]2*s*( 1.38)2*p*( 4.05)3*p*( 0.01)3*d*( 0.01)** | **-0.44875** | **-0.439267** |

| | | | |
|---|---|---|---|
| **O1** | **[core]2*s*( 1.70)2*p*( 4.87)3*d*( 0.01)** | **-0.58076** | **-0.484648** |
| *Cis*-I (2,4′-Hpcad) | | | |
| **N1** | **[core]2*s*( 1.38)2*p*( 4.04)3*p*( 0.01)3*d*( 0.01)** | **-0.44190** | **-0.424591** |
| N2 | [core]2*s*( 1.25)2*p*( 4.21)3*p*( 0.01) | -0.48111 | -0.434042 |
| **N3** | **[core]2*s*( 1.39)2*p*( 3.84)3*p*( 0.01)3*d*( 0.01)** | **-0.25553** | **-0.267533** |
| N4 | [core]2*s*( 1.37)2*p*( 4.52)3*p*( 0.01) | -0.90095 | -0.655540 |
| **N5** | **[core]2*s*( 1.37)2*p*( 4.03)3*p*( 0.01)3*d*( 0.01)** | **-0.41440** | **-0.443883** |
| **O1** | **[core]2*s*( 1.70)2*p*( 4.86)3*d*( 0.01)** | **-0.57414** | **-0.477773** |

## Single Crystal X-Ray Diffraction

**Table S3.** Crystallographic Data for compounds **1**and **2.**

| Compound | **1** | **2** |
|---|---|---|
| Empirical formula | $C_{32}H_{44}Dy_2N_{10}O_{16}$ | $C_{32}H_{36}Dy_2N_{10}O_{12}$ |
| Formula weight | 1149.77 | 1077.71 |
| Temperature | 296 K | 296 K |
| Crystal system | Monoclinic | Monoclinic |
| space group | *C*2/c | $P2_1/n$ |
| *a* (Å) | 17.6569(7) | 11.392(2) |
| *b* (Å) | 13.0716(5) | 14.396(2) |
| *c* (Å) | 18.0859(7) | 11.488(2) |
| *α* (°) | 90 | 90 |
| *β* (°) | 97.960(4) | 102.493(3) |
| *γ* (°) | 90 | 90 |
| *V* (Å$^3$) | 4134.1(3) | 1839.4(5) |
| *Z* | 4 | 2 |
| *F*(000) | 2264.0 | 1052.0 |
| Goodness-of-fit on *F*^2 | 0.946 | 1.158 |
| Final *R* indices [*I*>2sigma(*I*)] | *R*1 = 0.0418<br>*wR*2 = 0.1129 | *R*1 = 0.0740<br>*wR*2 = 0.1724 |
| *R* indices (all data) | *R*1 =0.0634<br>*wR*2 = 0.1290 | *R*1 = 0.0902<br>*wR*2 = 0.1806 |
| CCDC | 1523394 | 1469449 |

**Table S4.** Selected bond lengths (Å) and angles (°) for **1**and **2.**

| **1** | | **2** | |
|---|---|---|---|
| Dy1-O1 | 2.350(4) | Dy1-O4 | 2.610(9) |
| Dy1-O5 | 2.352(4) | Dy1-O1 | 2.306(9) |

| | | | |
|---|---|---|---|
| Dy1-O6 | 2.363(4) | Dy1-O4$^{i}$ | 2.346(8) |
| Dy1-O3 | 2.452(5) | Dy1-O5 | 2.382(8) |
| Dy1-O2 | 2.434(5) | Dy1-N1 | 2.425(1) |
| Dy1-N3 | 2.430(5) | Dy1-O7 | 2.433(1) |
| Dy1-O17$^{i}$ | 2.450(5) | Dy1-O2 | 2.454(9) |
| Dy1-N5 | 2.575(3) | Dy1-O6 | 2.473(1) |
| Dy1-O6$^{i}$ | 2.617(4) | Dy1-N2 | 2.503(1) |
| O2-Dy1-O17$^{i}$ | 75.61(2) | O5-Dy1-O2 | 77.0(3) |
| N3-Dy1-O17$^{i}$ | 137.9(2) | N1-Dy1-O2 | 75.8(4) |
| O1-Dy1-N5 | 127.68(1) | O7-Dy1-O2 | 150.5(3) |
| O5-Dy1-N5 | 77.30(1) | O1-Dy1-O6 | 125.2(4) |
| O6-Dy1-N5 | 88.70(4) | O4$^{i}$-Dy1-O6 | 80.4(4) |
| O3-Dy1-N5 | 72.14(2) | O5-Dy1-O6 | 71.5(3) |
| O2-Dy1-N5 | 85.66(2) | N1-Dy1-O6 | 115.7(4) |
| N3-Dy1-N5 | 62.66(1) | O7-Dy1-O6 | 51.4(3) |
| O17$^{i}$-Dy1-N5 | 145.61(2) | O6-Dy1-O4 | 134.7(3) |
| O1-Dy1-O6$^{i}$ | 74.11(1) | N2-Dy1-O4 | 123.3(3) |
| O6-Dy1-O6$^{i}$ | 66.25(15) | O1-Dy1-O4$^{i}$ | 75.3(3) |
| O3-Dy1-O6$^{i}$ | 113.48(2) | O1-Dy1-O5 | 145.0(3) |
| O2-Dy1-O6$^{i}$ | 125.22(2) | O4$^{i}$-Dy1-O5 | 78.4(3) |
| O1-Dy1-O5 | 145.11(1) | O1-Dy1-N1 | 64.5(3) |
| O1-Dy1-O6 | 83.81(2) | O4$^{i}$-Dy1-N1 | 138.8(4) |
| O5-Dy1-O6 | 71.86(2) | O5-Dy1-N1 | 141.6(3) |
| O1-Dy1-O3 | 132.40(2) | O1-Dy1-O7 | 79.8(3) |
| O5-Dy1-O3 | 71.97(2) | O4$^{i}$-Dy1-O7 | 89.3(3) |
| O6-Dy1-O3 | 141.93(2) | O5-Dy1-O7 | 122.8(3) |
| O1-Dy1-O2 | 85.09(2) | N1-Dy1-O7 | 75.9(4) |
| O5-Dy1-O2 | 124.45(2) | O1-Dy1-O2 | 95.2(3) |
| O6-Dy1-O2 | 160.70(2) | O4$^{i}$-Dy1-O2 | 117.7(3) |
| O3-Dy1-O2 | 52.48(2) | O2-Dy1-O6 | 139.4(4) |
| O1-Dy1-N3 | 65.02(2) | O1-Dy1-N2 | 128.4(4) |
| O5-Dy1-N3 | 132.40(2) | O4$^{i}$-Dy1-N2 | 154.0(4) |
| O6-Dy1-N3 | 82.08(2) | N1-Dy1-O4 | 109.5(3) |
| O3-Dy1-N3 | 114.91(2) | O7-Dy1-O4 | 150.6(3) |
| (i) -*x*+1/2, -*y*+3/2, -*z*+1. | | (i) 1-*x*, 1-*y*, 1-*z*. | |

## Thermogravimetric analysis

As shown in Figure S5a, the TGA curve of compound **1** suggests the first weight loss of 6.2% in range of 30 °C – 140 °C, corresponding to loss of two lattice water molecules and two coordinated water molecules (Calcd. 6.4%). It is highly possible that 1 would firstly lose two lattice water molecules due to the grinding before measurement when compared to the result of crystal

measurement. The framework decomposes gradually as the temperature increasing. For compound **2**, the decomposition begins at 184 °C, then weight loss (4.6%) in the range of 184 to 195 °C, which larger than the content of coordinated water molecules (Calcd. 3.2%), likely due to partial decomposition of coordinated groups in compound **2**, after which the framework decomposes gradually.

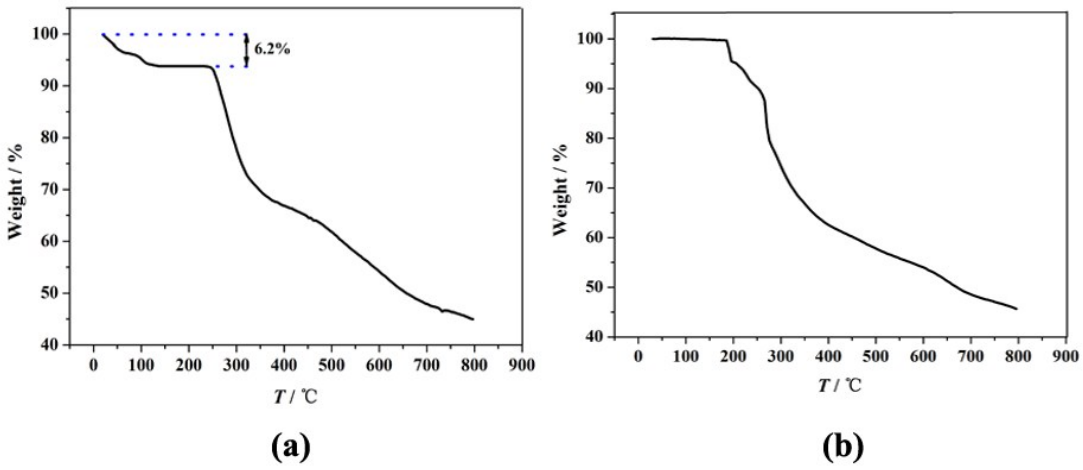


**Figure S5.** TGA of **1**(a) and **2**(b) under dry $N_2$ atmosphere.

## X-Ray Powder Diffraction

The simulated PXRD pattern was calculated using single-crystal X-ray diffraction data and processed by Mercury 2.4[S4] program provided by the Cambridge Crystallographic Data Center.

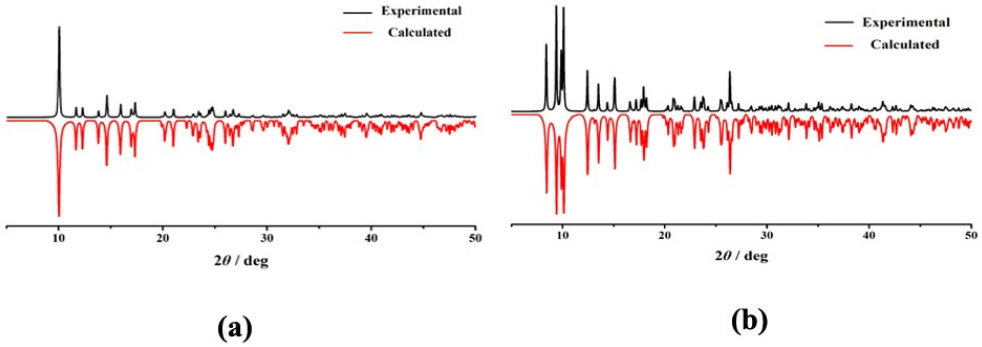


**Figure S6.** Experimental PXRD and calculated PXRD of **1**(a) and **2**(b).

## Crystal Structure

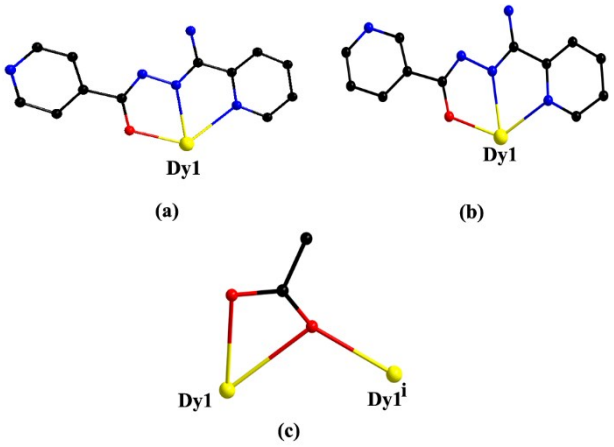


**Figure S7**. (a) Connection mode of 2,4′-Hpcad ligand; (b) Connection mode of 2,3′-Hpcad ligand; Three coordinate modes of acetate groups: (c) $\eta^1$:$\eta^2$:$\mu_2$.

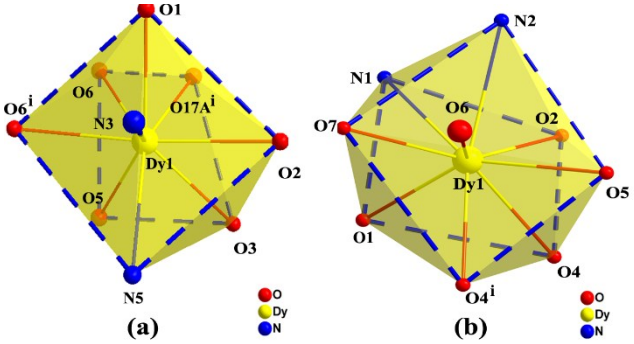


**Figure S8.** Local coordination geometry of the $Dy^{III}$ ion in **1**(a)) and **2**(b).

**Table S5.** The calculated results for $Dy^{III}$ ions configuration of **1** and **2** by SHAPE 2.1 software.

| Configuration | ABOXIY, **1** | ABOXIY, **2** |
|---|---|---|
| Octagonal pyramid ($C_{8v}$) | 22.964 | 22.322 |
| Heptagonal bipyramid ($D_{7h}$) | 17.399 | 17.698 |
| Johnson Triangular cupola J3 ($C_{3v}$) | 13.355 | 14.214 |
| Capped Cube J8 ($C_{4v}$) | 9.623 | 9.942 |
| Spherical-relaxed capped Cube ($C_{4v}$) | 8.152 | 8.328 |
| Capped square antiprism J10 ($C_{4v}$) | 3.357 | 3.171 |
| **Spherical capped square antiprism ($C_{4v}$)** | **2.336** | **2.167** |
| Tricapped trigonal prism J51 ($D_{3h}$) | 3.230 | 3.542 |
| Spherical tricapped trigonal prism ($D_{3h}$) | **2.563** | **2.965** |
| Tridiminished icosahedron J63 ($C_{3v}$) | 10.847 | 11.178 |

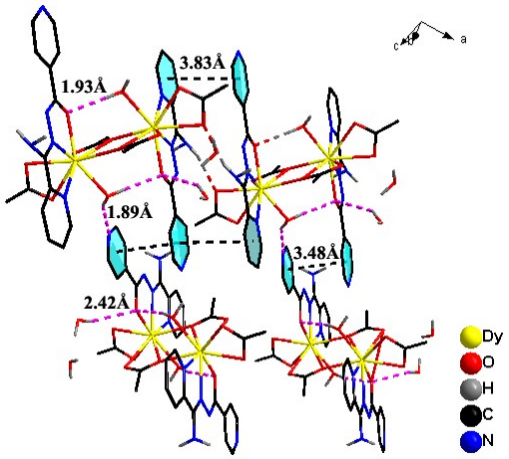


**Figure S9.** Packing diagram for compound **1**. The black dotted lines represent the $\pi\cdots\pi$ interactions, and the purple dotted lines represent the hydrogen bonding interactions.

**Table S6.** Hydrogen bond geometry in compound **1**.

| D-H···A | $d_{D\text{-}H}$/Å | $\boldsymbol{d_{H\cdots A}}$/Å | $d_{D\cdots A}$/Å | ∠ DHA° |
|---|---|---|---|---|
| O5-H5A···O1$^{i}$ | 0.89 | **1.93** | 2.807(5) | 167.5 |
| O5-H5B···N1$^{vi}$ | 0.89 | **1.89** | 2.696(6) | 149.3 |
| O9-H9A···O1$^{ii}$ | 0.85 | **2.42** | 3.159(1) | 146.6 |

(i) -x+1/2,-y+3/2,-z+1; (ii) x+1/2,y-1/2,z; (iii) -x,-y+2,-z+1; (iv) x+1/2,-y+3/2,z+1/2

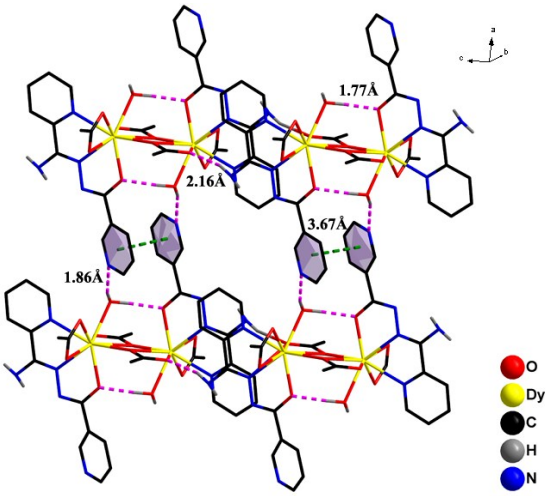


**Figure S10.** Packing diagram for compound **2**. The black dotted lines represent the $\pi\cdots\pi$ interactions, and the purple dotted lines represent the hydrogen bonding interactions.

**Table S7.** Hydrogen bond geometry in compound **2**.

| D-H···A | $d_{D-H}$/Å | $\boldsymbol{d_{H\cdots A}}$/Å | $d_{D\cdots A}$/Å | ∠ DHA° |
|---|---|---|---|---|
| O5-H5A···O1$^{i}$ | 0.96 | **1.77** | 2.721 (1) | 169.1 |
| O5-H5B···N5$^{v}$ | 0.96 | **1.86** | 2.757 (1) | 155.3 |
| N4-H4B···O2$^{iii}$ | 0.89 | **2.16** | 3.014 (1) | 161.2 |

(i) 1-x, 1-y, 1-z; (ii) -1+x, y, z; (iii) 1-x, 1-y, 2-z; (iv) -x, 1-y, 1-z; (v) 1+x, y, z.

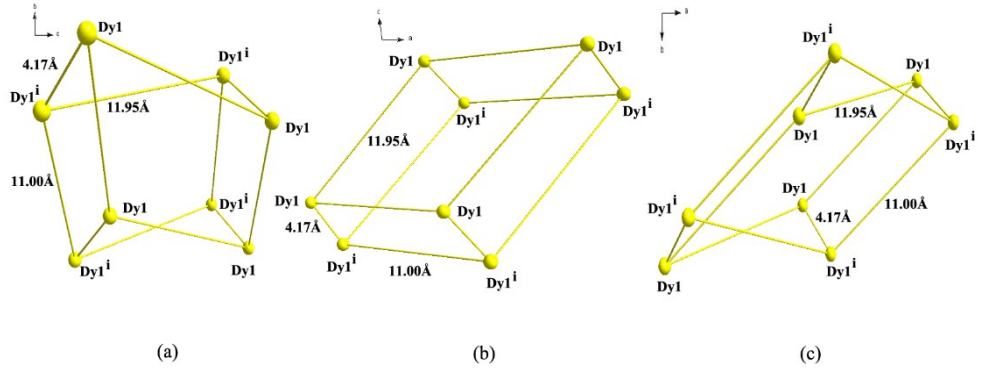


**Figure S11.** The distances of dinuclear Dy units in compound **1**. (a) along the *a* axis; (b) along the *b* axis; (c) along the *c* axis.

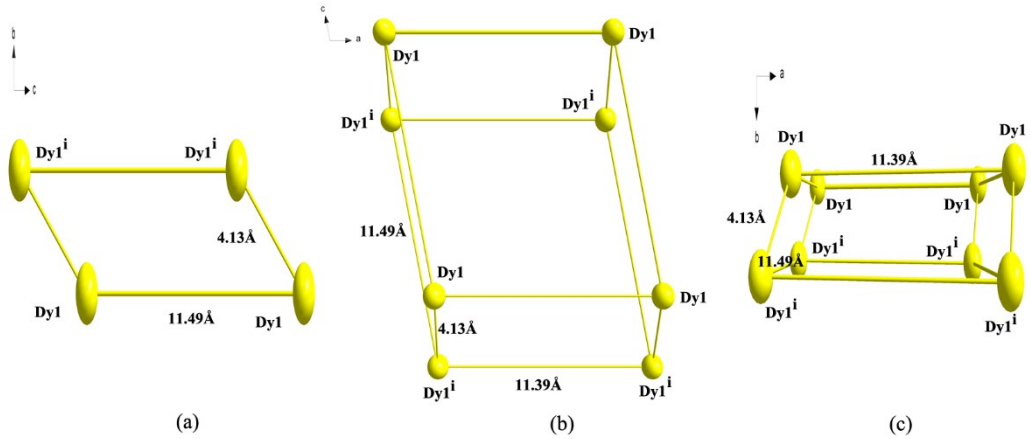


**Figure S12.** The distances of dinuclear Dy units in compound **2**. (a) along the *a* axis; (b) along the *b* axis; (c) along the *c* axis.

## Magnetic Measurements

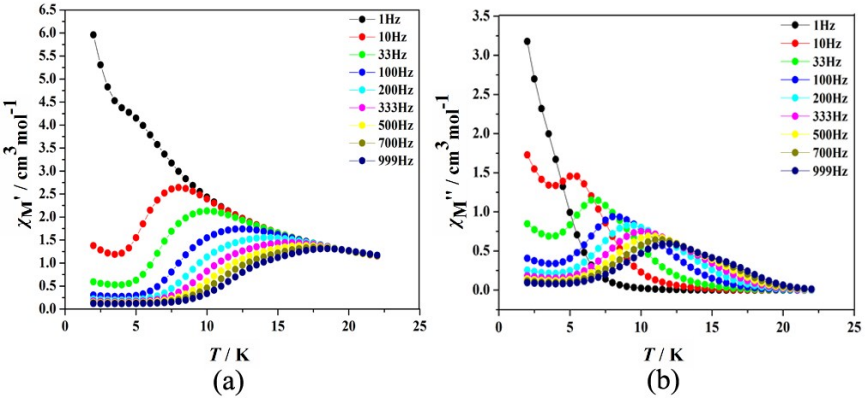


**Figure S13.** Frequency dependence of the in-phase (a) and out-of phase (b) ac susceptibility signals under 0 Oe for **1**.

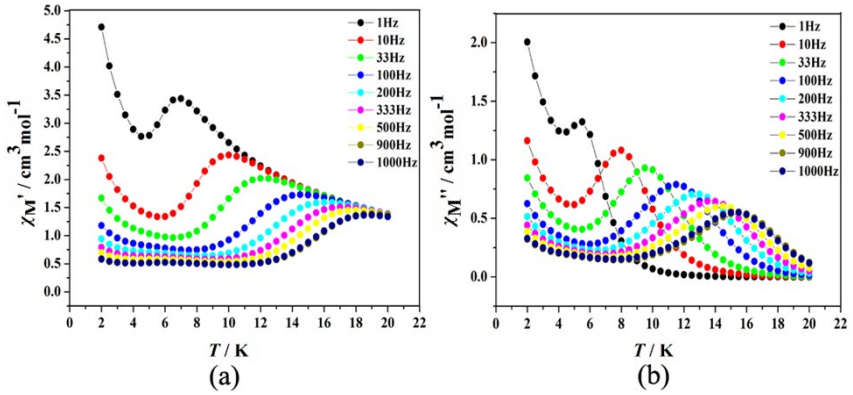


**Figure S14.** Temperature dependence of the in-phase (a) and out-of phase (b) ac susceptibility signals under 0 Oe dc field for **2**.

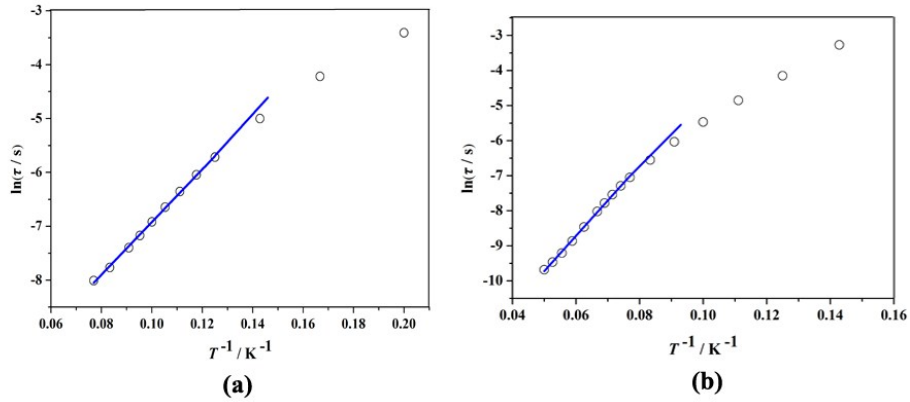


**Figure S15.** Plot of the relaxation time $\tau$ (T) (logarithmic scale) versus $T^{-1}$ for **1**(a) and **2**(b); the solid blue line corresponds represents fitting to the Orbach relaxation process ($U_{eff}$ = 48.9 K and a pre-exponential factor ($\tau_o$) = 7.4 x $10^{-6}$ s for **1**; $U_{eff}$ = 100.7 K and a pre-exponential factor ($\tau_o$) = 3.9 x $10^{-7}$ s for **2**).

**Table S8**. Relaxation fitting parameters from Least-Squares Fitting of $\chi(\omega)$ data of **1**.

| $T$(K) | $\Delta\chi_1$ ($cm^3mol^{-1}$) | $\Delta\chi_2$ ($cm^3mol^{-1}$) | $\alpha$ | $R^2$ |
|---|---|---|---|---|
| 5.0 | 4.87371 | 0.08822 | 0.23995 | 0.9999 |
| 6.0 | 4.06221 | 0.07437 | 0.22797 | 0.9989 |
| 7.0 | 3.49498 | 0.05875 | 0.22613 | 0.9944 |
| 8.0 | 3.06729 | 0.04944 | 0.22371 | 0.9880 |
| 8.5 | 2.89126 | 0.04873 | 0.22191 | 0.9830 |
| 9.0 | 2.73321 | 0.05304 | 0.21901 | 0.9814 |
| 9.5 | 2.59261 | 0.06379 | 0.21550 | 0.9801 |
| 10.0 | 2.46561 | 0.08472 | 0.20998 | 0.9851 |
| 10.5 | 2.35046 | 0.12035 | 0.20209 | 0.9867 |
| 11.0 | 2.05977 | 0.34295 | 0.15427 | 0.9872 |
| 12.0 | 1.90299 | 0.53988 | 0.10944 | 0.9845 |

**Table S9**. Relaxation fitting parameters from Least-Squares Fitting of $\chi(\omega)$ data of **2**.

| $T$(K) | $\Delta\chi_1$ ($cm^3mol^{-1}$) | $\Delta\chi_2$ ($cm^3mol^{-1}$) | $\alpha$ | $R^2$ |
|---|---|---|---|---|
| 7.0 | 3.47096 | 0.5908 | 0.21977 | 0.9908 |
| 8.0 | 2.96569 | 0.5240 | 0.16732 | 0.9856 |
| 9.0 | 2.62051 | 0.47874 | 0.13184 | 0.9850 |
| 10.0 | 2.68744 | 0.47427 | 0.11644 | 0.9842 |
| 11.0 | 2.44955 | 0.44061 | 0.10419 | 0.9852 |
| 12.0 | 2.25152 | 0.43836 | 0.08439 | 0.9898 |
| 13.0 | 2.08543 | 0.44576 | 0.07113 | 0.9929 |
| 13.5 | 1.77088 | 0.40845 | 0.06684 | 0.9931 |
| 14.0 | 1.94297 | 0.46796 | 0.06186 | 0.9951 |
| 14.5 | 1.65563 | 0.43595 | 0.05900 | 0.9958 |
| 15.0 | 1.82026 | 0.50771 | 0.05576 | 0.9962 |
| 16.0 | 1.71243 | 0.59232 | 0.03399 | 0.9960 |
| 17.0 | 1.61776 | 0.65061 | 0.03050 | 0.9880 |
| 18.0 | 1.53207 | 0.71282 | 0.02188 | 0.9888 |

## Results of *ab initio* investigation

The dinuclear compounds **1** and **2** have an inversion center, thus only one magnetic center is calculated. Complete-active-space self-consistent field (CASSCF) calculations on individual lanthanide $Dy^{III}$ fragment of the complete structure (see Figure S26 for the complete structures of compounds **1** and **2**) extracted from each compound on the basis of single-crystal X-ray determined geometry have been carried out with MOLCAS 8.0 program package.[S5] Each dysprosium center was calculated keeping the experimentally determined structure of the corresponding compound while replacing the neighboring $Dy^{III}$ ion by diamagnetic Lu.

The basis sets for all atoms are atomic natural orbitals from the MOLCAS ANO-RCC library: ANO-RCC-VTZP for $Dy^{III}$ ions; VTZ for close O and N; VDZ for distant atoms. The calculations employed the second order Douglas-Kroll-Hess Hamiltonian, where scalar relativistic contractions were taken into account in the basis set and the spin-orbit couplings were handled separately in the restricted active space state interaction (RASSI-SO) procedure. For the fragment of individual $Dy^{III}$ ions, active electrons in 7 active spaces include all *f* electrons (CAS(9 in 7)) in the CASSCF calculation. To exclude all the doubts, we calculated all the roots in the active space. We have mixed the maximum number of spin-free state which was possible with our hardware (all from 21 sextets, 128 from 224 quadruplets, 130 from 490 doublets for the $Dy^{III}$ fragment).

To fit the exchange interactions in these complexes, we took two steps to obtain them. Firstly, we calculated one $Dy^{III}$ fragment using CASSCF to obtain the corresponding magnetic properties. Then, the exchange interaction between the magnetic centers is considered within the Lines model,[S6] while the account of the dipole-dipole magnetic coupling is treated exactly. The Lines model is effective and has been successfully used widely in the research field of f-element single-molecule magnets.[S7]

For each of compounds **1** and **2**, there is only one type of *J*.

The exchange Hamiltonian is:

$$\hat{H}_{exch} = -J_{total}\,\hat{S}_{Dy1}\,\hat{S}_{Dy1'} \qquad \text{(S1)}$$

The $J_{total}$ is the parameter of the total magnetic interaction ($J_{total} = J_{diploar} + J_{exchange}$) between magnetic center ions. The $\hat{S}_{Dy} = \pm 1/2$ are the ground pseudospin on the $Dy^{III}$ sites. The dipolar magnetic coupling can be calculated exactly, while the exchange coupling constants were fitted through comparison of the computed and measured magnetic susceptibility and molar magnetization using the POLY_ANISO program.[S8]

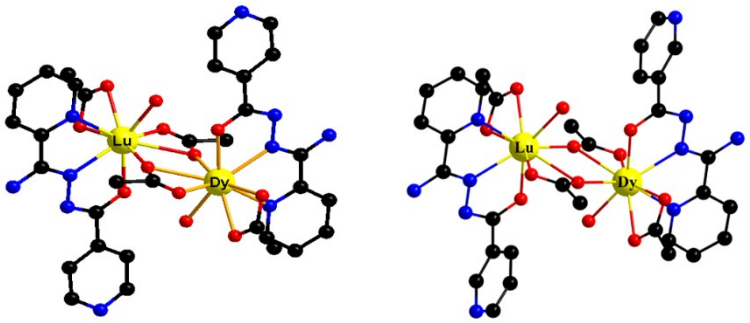


(a) (b)

**Figure S16**. Calculated complete structures for compounds **1**(a) and **2**(b); H atoms are omitted.

**Table S10**. Calculated energy levels ($cm^{-1}$), $\boldsymbol{g}$ ($g_x$, $g_y$, $g_z$) tensors and $m_J$ values of the lowest Kramers doublets (KDs) of one $Dy^{III}$ center for compounds **1** and **2**.

| KD | 1 | | | 2 | | |
|---|---|---|---|---|---|---|
| | ***E*/cm$^{-1}$** | ***g*** | ***m*$_J$** | ***E*/cm$^{-1}$** | ***g*** | ***m*$_J$** |
| 1 | 0.0 | 0.004<br>0.028<br>19.617 | ±15/2 | 0.0 | 0.022<br>0.032<br>19.581 | ±15/2 |
| 2 | **104.4** | 0.026<br>0.114<br>19.331 | ±11/2 | **121.9** | 0.864<br>1.681<br>16.071 | ±13/2 |
| 3 | 149.9 | 0.099<br>0.530<br>15.476 | ±13/2 | 158.1 | 0.823<br>2.360<br>11.755 | ±1/2 |
| 4 | 187.3 | 3.568<br>5.058<br>12.760 | ±9/2 | 178.8 | 1.960<br>4.030<br>11.429 | ±7/2 |
| 5 | 236.8 | 1.243<br>2.497<br>11.104 | ±3/2 | 212.7 | 0.065<br>4.930<br>11.190 | ±9/2 |
| 6 | 326.7 | 0.498<br>0.655<br>17.400 | ±7/2 | 266.0 | 2.639<br>4.442<br>9.446 | ±5/2 |
| 7 | 349.1 | 0.429<br>0.778<br>16.295 | ±5/2 | 315.8 | 1.256<br>2.753<br>14.582 | ±11/2 |
| 8 | 488.6 | 0.064<br>0.095<br>19.025 | ±1/2 | 422.4 | 0.175<br>0.191<br>19.101 | ±3/2 |

**Table S11.** Exchange energies ($cm^{-1}$) and main values of the $g_z$ for the lowest two exchange doublets of compounds **1**and **2**.

| | **1** | | **2** | |
|---|---|---|---|---|
| | *E* | $g_z$ | *E* | $g_z$ |
| 1 | 0.0 | 0.000 | 0.0 | 0.000 |
| 2 | 0.6 | 39.229 | 1.6 | 39.158 |

**Table S12.** Natural Bond Order (NBO) charges per atoms in the ground state of compounds **1** and **2** calculated within CASSCF.

| **1** | | **2** | |
|---|---|---|---|
| Dy1 | 2.514 | Dy1 | 2.514 |
| O6 | −0.748 | O4$^{i}$ | −0.753 |
| O6$^{i}$ | −0.683 | O4 | −0.690 |
| O17$^{i}$ | −0.681 | O2 | −0.740 |
| **O1** | −0.839 | **O1** | **−0.840** |
| O2 | −0.799 | O7 | −0.757 |
| **O3** | −0.805 | **O6** | **−0.755** |
| **O5** | −0.744 | **O5** | **−0.766** |
| **N3** | −0.314 | **N1** | **−0.350** |
| N5 | −0.371 | N2 | −0.341 |
| (i) -*x*+1/2, -*y*+3/2, -*z*+1. | | (i) 1-*x*, 1-*y*, 1-*z*. | |

## References


[S1] Frisch, M. J. et al. Gaussian 09, Revision E.01; Gaussian Inc: Wallingford, CT, 2009.

[S2] Becke A D. *J. Chem. Phys.*, **1993,** 98:5648-5652

[S3] Lee C, Yang W, Parr R G, et al. *Phys. Rev. B.*, **1988,** 37:785-789

[S4] C. F. Macrae, I. J. Bruno, J. A. Chisholm, P. R. Edgington, P. McCabe, E. Pidcock, L. Rodriguez-Monge, R. Taylor, J. van de Streek, P. A. Wood, *J. Appl. Crystallogr.,* **2008**, 41, 466.

[S5] Karlström, G.; Lindh, R.; Malmqvist, P.-Å.; Roos, B. O.; Ryde, U.; Veryazov, V.; Widmark, P.-O.; Cossi, M.; Schimmelpfennig, B.; Neogrady, P.; Seijo, L. MOLCAS: a Program Package for Computational Chemistry. *Comput. Mater. Sci*. **2003**, *28*, 222.

[S6] Lines, M. E. *J. Chem. Phys*. **1971**, *55*, 2977.

[S7] (a) Mondal, K. C.; Sundt, A.; Lan, Y. H.; Kostakis, G. E.; Waldmann, O.; Ungur, L.; Chibotaru, L. F.; Anson, C. E.; Powell, A. K. *Angew. Chem. Int. Ed*. **2012**, *51*, 7550. (b) Langley, S. K.; Wielechowski, D. P.; Vieru, V.; Chilton, N. F.; Moubaraki, B.; Abrahams, B. F.; Chibotaru, L. F.; Murray, K. S. *Angew. Chem. Int. Ed*. **2013**, *52*, 12014.

[S8] (a) Chibotaru, L. F.; Ungur, L.; Soncini, A. *Angew. Chem. Int. Ed.*, **2008**, *47*, 4126. (b) Ungur, L.; Van denHeuvel, W.; Chibotaru, L.F. *New J. Chem.*, **2009**, *33*, 1224. (c) Chibotaru, L. F.; Ungur, L.; Aronica,C.; Elmoll, H.; Pilet, G.; Luneau, D. *J. Am. Chem. Soc.*, **2008**, *130*, 12445.